4. V. Ya. Arsenin, Mathematical Physics [in Russian], Nauka, Moscow (1966).
5. N. S. Koshlyakov, É. B. Gliner, and M. M. Smirnov, Equations in Partial Derivatives in Mathematical Physics [in Russian], Vysshaya Shkola, Moscow (1970).
6. S. K. Godunov and V. S. Ryaben'kii, Difference Schemes [in Russian], Nauka, Moscow (1973).
7. V. M. Kolobashkin and V. I. Selyakov, "Fluid infiltration in a stratified medium," Gaz. Prom., No. 6 (1980).

PROPAGATION OF NONLINEAR COMPRESSION PULSES IN GRANULAR MEDIA

V. F. Nesterenko

UDC 624.131 + 532.215 + 534.22

The study of mechanics of a granular medium is of substantial interest, both scientifically and for the solution of applied problems. Such materials are, for example, good buffers for shock loads. Their study is important for the development of processes of the pulse deformation of several porous materials. A review of studies of small deformations and elastic wave propagation in these media was carried out in [1] on the basis of discrete models. The structure of a stationary shock wave was analyzed in [2] as a function of its amplitude.

1. Statement of the Problem. The problem of nonstationary, nonlinear perturbations in one-dimensional granular media is stated in the present paper on the basis of the well-known interaction between neighboring granules.

As an interaction law we choose the Hertz law [3]

$$F = \frac{2E}{3(1-\nu^2)}\left(\frac{R_1R_2}{R_1+R_2}\right)^{1/2}\{(R_1+R_2)-(x_2-x_1)\}^{3/2}, \tag{1.1}$$

where F is the compression force of granules, E is the Young modulus of their material, R_1 and R_2 are radii, ν is the Poisson coefficient, and x_1 and x_2 are the coordinates of spherical granules ($x_2 > x_1$).

It is necessary to point out that a dependence of the form $\delta^{3/2}$, where δ is the closest approach of particle centers, is valid not only for spheres, but also for contacts of other finite bodies [3]. Interestingly, it is only due to the finite particle sizes of a linearly elastic material constituting the granular medium that its behavior has a nonlinearly elastic character.

The use of the static Hertz law in solving dynamic problems implies the following restrictions: 1) the maximum stress achieved at the center of the contact must be less than the elastic limit; 2) the sizes of the contact surface are much smaller than the radii of curvature of each particle; and 3) the characteristic times of the problem τ are much longer than the oscillation period of the basic shape for the elastic sphere T

$$\tau \gg T \approx 2.5R/c_1,$$

where c_1 is the velocity of sound in the sphere material.

Conditions 1-3 restrict the mass velocities of the medium to quantities of the order of several meters per second for metallic particles with radii in the interval 1-5 mm. Dissipation processes are not taken into account at the present stage of the study.

For numerical study of perturbation propagation processes in a one-dimensional chain of spherical particles with arbitrary radii R_i the second order equations of motion were reduced to a first order system of equations:

$$\dot{x}_i = F_i(\mathbf{x}),\ \mathbf{x} = (x_1, x_2, \ldots, x_{2N}),\ i = 1, \ldots, 2N, \tag{1.2}$$
$$F_i(\mathbf{x}) = \varphi_i(\mathbf{x}) - \psi_i(\mathbf{x}),\ i = 1, \ldots, N,$$

Novosibirsk. Translated from Zhurnal Prikladnoi Mekhaniki i Tekhnicheskoi Fiziki, No. 5, pp. 136-148, September-October, 1983. Original article submitted April 12, 1982.

0021-8944/83/2405-0733$07.50

$$F_i(\mathbf{x}) = x_{i-N},\ i = N+1, \ldots, 2N,$$
$$\varphi_i(\mathbf{x}) = \left(\frac{R_iR_{i-1}}{R_i+R_{i-1}}\right)^{1/2} \frac{E}{2\pi\rho_0(1-\nu^2)R_i^3}\delta_{i-1}^{3/2}, \quad \text{if} \quad \delta_{i-1} > 0, \quad i = 2, \ldots, N,$$
$$\varphi_i(\mathbf{x}) = 0, \quad \text{if} \quad \delta_{i-1} \leqslant 0, \quad i = 2, \ldots, N, \tag{1.2}$$
$$\psi_i(\mathbf{x}) = \left(\frac{R_iR_{i-1}}{R_i+R_{i+1}}\right)^{1/2} \frac{E}{2\pi\rho_0(1-\nu^2)R_i^3}\delta_i^{3/2}, \quad \text{if} \quad \delta_i > 0, \quad i = 1, \ldots, N-1,$$
$$\psi_i(\mathbf{x}) = 0, \quad \text{if} \quad \delta_i \leqslant 0, \quad i = 1, \ldots, N-1,$$
$$\delta_{i-1} = R_i + R_{i-1} - (x_{N+i} - x_{N+i-1}), \quad i = 2, \ldots, N,$$
$$x_{N+i}\ (t=0) = x_{N+i-1} + R_i + R_{i-1}, \quad i = 2, \ldots, N, \quad x_{N+1}(t=0) = 0.$$

It is clear from this form of writing that for $N \geqslant i \geqslant 1$ the quantities x_i are the velocity values of the i-th particle, while for $2N \geqslant i > N$ they are the coordinate values. The initial conditions for the velocities on φ_1 and ψ_N are specified below for each separate case.

2. Analysis of the Anharmonic and Long-Wave Approximations. Consider a one-dimensional chain of identical spherical granules. We assume that it is subject to constant compression forces F_0, applied to the chain edges and securing the initial closest approach δ_0. As will be clear from the following, δ_0 is conveniently introduced into the equation explicitly. With this purpose in mind we replace the coordinate x_i by the displacement of the given particle from its equilibrium position u_i. Using the expression for the force (1.1), the particle equation of motion becomes

$$\ddot{u}_i = A(\delta_0 - u_i + u_{i-1})^{3/2} - A(\delta_0 - u_{i+1} + u_i)^{3/2},$$
$$A = E(2R)^{1/2}/[3(1-\nu^2)m], \quad N-1 \geqslant i \geqslant 2, \tag{2.1}$$

where m is the mass of the particle. It is assumed here that the distance between the particle centers does not exceed 2R.

The equation provided will describe the propagation of one-dimensional perturbations in a three-dimensional simple cubic packing of spheres if the front plane is parallel to the cube boundaries. Differences occur only in the numerical coefficient in A.

Equation (2.1) can be transformed to a well-investigated system of nonlinear oscillators under the assumption of small deformation in the medium by comparison with the initial closest approach δ_0, i.e., putting

$$|u_{i-1} - u_i|/\delta_0 \ll 1.$$

In the anharmonic approximation Eq. (2.1) is then

$$\ddot{u}_i = \alpha(u_{i+1} - 2u_i + u_{i-1}) + \beta(u_{i+1} - 2u_i + u_{i-1})\times$$
$$\times(u_{i-1} - u_{i+1}), \tag{2.2}$$
$$\alpha = \frac{3}{2}A\delta_0^{1/2}, \quad \beta = \frac{3}{8}A\delta_0^{-1/2}, \quad N-1 \geqslant i \geqslant 2.$$

Equations of the type (2.2) with a quadratic nonlinearity were solved numerically in a number of studies (see, e.g., [4, 5]), and a brief review can be found in [6]. It was shown that in the problem of a piston moving with a constant velocity v_0 there exists an oscillating nonstationary structure of a "shock wave," in whose head is formed a soliton with the velocity in the maximum equal to $2v_0$. The oscillations are damped behind the front even in the absence of dissipation. A similar equation can be obtained for small perturbations and for a different choice of interaction potentials. Oscillations undamped in time were observed near the piston for sufficiently high values of its velocity in numerical calculations of a Toda chain with a particle interaction determined by the Morse potential [6, 7]. The existence of solitons in a chain with a Morse potential was shown numerically in [7].

In the long-wave approximation ($L \gg a = 2R$, where L is a characteristic spatial size of the perturbation) and with the usual replacement

$$u_i = u(x), \quad u_{i-1} = e^{-aD}u(x), \quad u_{i+1} = e^{aD}u(x),$$
$$D \equiv \partial/\partial x$$

one can obtain from Eq. (2.2) the nonlinear wave equation

$$u_{tt} = c_0^2 u_{xx} + 2c_0\gamma u_{xxxx} - \varepsilon u_x u_{xx},$$
$$c_0^2 = A\delta_0^{1/2}6R^2,\ \gamma = c_0R^2/6,\ \varepsilon = c_0^2R/\delta_0. \tag{2.3}$$

All terms of order $\frac{c_0^2u}{L}\left[\left(\frac{a}{L}\right)^4+\left(\frac{a}{L}\right)^2\left(\frac{u}{\delta_0}\right)^2\right]$ and higher were omitted in deriving Eq. (2.3).

Solutions of this equation satisfy the Korteweg–de Vries (KdV) equation, whose properties are quite well known [8], accurately up to terms quadratic in the nonlinearity and dispersion coefficients. Not dwelling on the details of discussing these properties, we note that in a granular medium of proper structure, compressed by an external force, the existence is possible of solitary waves, periodic waves, and shock waves with an oscillating structure. The qualitative behavior of the solutions depends on the time characteristics of the loading pulse [8].

We are interested in the case $\delta_0 \to 0$. Then, as seen from Eq. (2.2), the quantity $\beta \to \infty$, and the anharmonic approximation becomes inapplicable. For $\delta_0 = 0$, in the long-wave approximation compression waves of small amplitude cannot be described by the standard wave approximation, which is a direct consequence of the anharmonic approximation. In the case $|u_{i-1} - u_i|/\delta_0 \geqslant 1$ one can obtain from (2.1) only an equation corresponding to the long-wave approximation ($L >> a$) by a replacement similar to the preceeding one. The equation is

$$u_{tt} = c^2\left\{\frac{3}{2}(-u_x)^{1/2}u_{xx} + \frac{a^2}{8}(-u_x)^{1/2}u_{xxxx} - \frac{a^2u_{xx}u_{xxx}}{8(-u_x)^{1/2}} - \frac{a^2}{64}\frac{(u_{xx})^3}{(-u_x)^{3/2}}\right\}, \tag{2.4}$$
$$-u_x > 0,\quad c^2 = \frac{2E}{\pi\rho_0(1-\nu^2)}.$$

In the equation given the displacement u includes the initial displacement responsible for the closest approach δ_0. The three last terms in Eq. (2.4) are of order $(a/L)^2$ in comparison with the first. Higher-order terms have been omitted. In the presence of a constant compression force, guaranteeing an initial closest approach δ_0, Eq. (2.4) reduces to the nonlinear equation (2.3) in the same approximation. This is easily done by representing the full deformation in the form

$$u_x = -\delta_0/2R + \Delta u_x$$

and carrying out an expansion in the small quantity Δu_x of the terms in the right-hand side of the equation. Standard solutions of Eq. (2.4) can be found in the form $u(x - Vt)$. Introducing the new variable $\xi = -u_x$, we obtain

$$\frac{V^2}{c^2}\xi_x = \frac{3}{2}\xi^{1/2}\xi_x + \frac{a^2}{8}\frac{(\xi\xi_{xx})_x}{\xi^{1/2}} - \frac{a^2\xi_x^3}{64\xi^{3/2}}. \tag{2.5}$$

Equation (2.5) can be integrated, performing the variable replacement $\xi = z^{4/5}$:

$$\frac{V^2}{c^2}z^{4/5} = z^{6/5} + \frac{a^2}{10}z^{1/5}z_{xx} + C_1$$

(C_1 is an integration constant). The last equation is conveniently written in dimensionless form, with variable replacement:

$$z = \left(\frac{V}{c}\right)^5 y,\quad x = \frac{a}{\sqrt{10}}\left(\frac{V}{c}\right)^{-5/2}\eta, \tag{2.6}$$
$$y^{4/5} = y^{6/5} + y^{1/5}y_{\eta\eta} + C_2$$

(C_2 is a constant).

If $C_2 = 0$, Eq. (2.6) is easily integrated. In a system moving with velocity V the solution is

$$\xi = \left(\frac{5}{4}\frac{V^2}{c^2}\right)^2\cos^4\frac{\sqrt{10}}{5a}x. \tag{2.7}$$

For $x = \frac{5a}{\sqrt{10}}\left(\frac{\pi}{2} \pm \pi n\right)$, $n=0, 1, \ldots$ ξ vanishes. This is found to contradict the condition $\xi > 0$, under which Eq. (2.4) was derived. Therefore it is necessary to study the behavior of the solution for $C_3 \neq 0$. With this purpose in mind we rewrite Eq. (2.6) in the following form, making it possible to use the analogy with particle motion in the potential field [8]:

$$y_{\eta\eta} = -\frac{\partial}{\partial y} W(y), \; W(y) = -\frac{5}{8} y^{8/5} + \frac{1}{2} y^2 + C_3 y^{4/5}.$$

It can be noted from the equation for W(y) that for $0 < C_3 < 5/27$ the function W(y) has the form of a curve with two extrema, shown in Fig. 1 for the values $C_3 = 4/27$ (curve 1) and 0.1 (curve 2). The extrema y_1 and y_2, marked on Fig. 1, correspond to the case $C_3 = 0.1$. For $C_3 \to 0$ the value of the maximum $W(y_1)$ also tends to zero, as does the value of its coordinate y_1. For $C_3 = 0$ we obtain a solution of (2.7) in the form of periodic waves. The deviation of C_3 from zero changes the nature of the solution qualitatively. From the shape of the function W(y) for $0 < C_3 < 5/27$ it can be concluded that Eq. (2.4) admits in this case the existence of stationary solutions of the type of periodic functions, while solitary waves are also possible under certain conditions. Indeed, near the maximum y_1 W(y) can be expanded in powers of $(y - y_1)$:

$$W(y) \approx W(y_1) - d(y - y_1)^2.$$

This form of potential energy leads within the mechanical analogy to an infinite "time" of particle fall with total energy $W(y_1)$ at the point y_1, which corresponds to the formation of a solitary wave [8]. The dependence of the potential energy on coordinate near y_1 corresponds to the stationary case for the KdV equation near the analog point. Therefore, the behavior of the solution for $y \to y_1$ will coincide asymptotically with the soliton solution of the KdV equation.

The restriction $C_3 < 5/27$ guarantees a value of the phase velocity of a solitary compression wave larger than the initial velocity of sound. Indeed, the phase velocity of a soliton V and the velocity of sound c_0 equal, respectively:

$$V = c\xi_0^{1/4} y_1^{-1/5}, \quad c_0 = c\xi_0^{1/4}\left(\frac{3}{2}\right)^{1/2},$$

where ξ_0 is the initial deformation. By comparing the expressions above it is seen that the inequality $V > c_0$ is satisfied for $y_1 < (2/3)^{5/2}$. The given condition is satisfied for $C_3 < 5/27$, as can be seen from the shape of W(y). For $C_3 = 5/27$ we have $y_1 = (2/3)^{5/2}$. The constant C_3 determines the ratio of the maximum soliton amplitude to the initial deformation ξ_0.

We find the soliton parameters corresponding to the case of small values $C_3 \ll 5/27$. If the value of the total particle energy equals in this case $W(y_1)$, the behavior of the solution for $y \gg y_1$ is near the behavior of the solution (2.7), corresponding to the case $C_3 = 0$ and to vanishing total energy. Consequently, the maximum deformation value in a solitary wave is near the amplitude value of the periodic wave (2.7):

$$\xi_m = \left(\frac{5}{4}\frac{V^2}{c^2}\right)^2.$$

The characteristic spatial size of a soliton is determined in this case by the period of the solution (2.7), which equals

$$L = \left(\frac{5a}{\sqrt{10}}\right)\pi \approx 5a.$$

The solitary waves found differ from solitons of the KdV equation by the dependence of the phase velocity on the wave amplitude. Another important difference is the independence of the characteristic spatial size of the soliton of Eq. (2.4) $L = 5a$ on the wave amplitude. As already noted, for a small deformation in the wave in comparison with ξ_0 the solution of Eq. (2.4) in the form of a solitary wave will be close to the analog solution of the KdV equation.

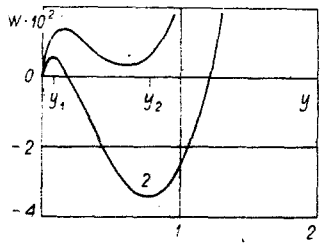

Fig. 1

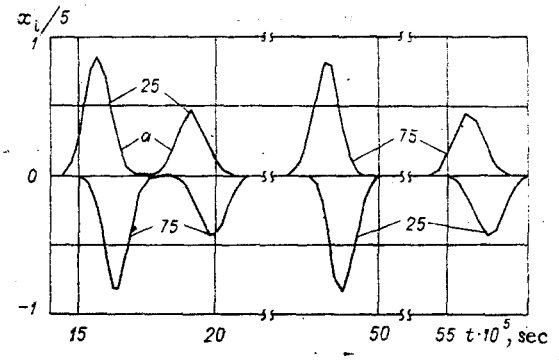

Fig. 2

In the presence of dissipation in the medium, for $C_3 = 0$ the deformation behind the front of the stationary shock wave corresponding to the minimum $W(y_1)$ equals the value ξ_c, coinciding with that found from the conservation laws for a chain with $\xi_0 = 0$:

$$\xi_c = V^4/c^4.$$

By comparing the quantities ξ_m and ξ_c it is seen that for weak dissipation the ratio of maximum deformation at the front of the stationary shock wave to its established value behind the front reaches the value

$$\xi_m/\xi_c = (5/4)^2 \approx 1.56.$$

The given difference in deformations leads to the circumstance that the ratio of the maximum pressure at the front of the stationary shock wave p_m to the established pressure behind it p_c can achieve the value

$$p_m/p_c = (\xi_m/\xi_c)^{3/2} = (5/4)^3 \approx 1.95.$$

Further use of the one-dimensional nonlinear chain of oscillators, interacting compressively according to the Hertz law, was carried out numerically.

3. Analysis of Computational Results. For numerical solution of the system of nonlinear equations (1.2) we used the Hamming and fourth order Runge–Kutta methods. The control solution was obtained by the momentum and energy conservation laws and comparison of the results obtained by various methods. During the calculation the momentum conservation law is satisfied with an accuracy not worse than 10^{-5}%, and total energy conservation law was satisfied within 10^{-3}–10^{-2}%. An estimate of the relative error in determining the particle velocity gives the value 10^{-2}%. With the purpose of verifying the correctness of the calculation we also compared the numerical solution of the problem of impact of a single particle with a chain of 100 identical particles, arranged with initial gaps, with its obvious exact solution. This comparison showed coincidence of the numerical and exact solutions within the limits of relative errors mentioned above.

We make one more comment. For $\delta_0 = 0$ and identical R_i Eq. (2.1) with variable replacement

$$w_i = \dot{u}_i/v_0, \quad \tau = t(A^2v_0)^{1/5}$$

is transformed to dimensionless form

$$\dot{w}_i = \left[\int_0^\tau (w_{i-1} - w_i)\,d\tau\right]^{3/2} - \left[\int_0^\tau (w_i - w_{i+1})\,d\tau\right]^{3/2}. \tag{3.1}$$

Clearly, for a chain with free ends ($\varphi_1 = \psi_N = 0$) identical τ values correspond to identical w_i values if the problem is solved with initial conditions

$$w_i(t=0) = 1,\ i = 1, \ldots, k,\ w_l(t=0) = 0,\ k < l \leqslant N.$$

A similar conclusion is also valid for solving the problem of a piston moving with constant velocity. Therefore, one further control method was verification of the observed equality of dimensionless particle velocity w_i at identical moments τ for problems with different values of initial velocities. For convenience of comparison with experiment the problem was

solved in real time. The choice of the initial step Δt in time was done by starting from the natural physical condition

$$\Delta t \ll T_1 = 2.94\,(5/8A)^{2/5}/v_0^{1/5},$$

where T_1 is the impact time of two spheres with relative initial velocity v_0 [3].

In the following the magnitude of the step was necessarily varied with the purpose of reaching a compromise between computational accuracy and computer time.

3.1. Decomposition of Initial Perturbation in a Chain of Granules with Free Ends. Here and later on (Secs. 3.2-3.4) all R_i are identical and equal to $3\cdot10^{-2}$ m. The following values were chosen for the quantities A and ρ_0, characteristic of steel particles: $A = 5.6\cdot10^{12}$ N/(m$^{3/2}$·kg), $\rho_0 = 7.8\cdot10^3$ kg/m^3. The initial conditions for velocity are the following in the first case:

$$x_i(t=0) = x_2(t=0) = v_0 = 5 \text{ m/sec}$$
$$x_i(t=0) = 0,\ N \geqslant i > 2,\ N = 100.$$

The time dependences obtained for x_i/v_0 are shown in Fig. 2 (curves *a*). It is seen that for these initial data two solutions are formed with practically resting material between them. The formation of an initial perturbation of two stationary solitary waves is already concluded on the twentieth particle. They further propagate as stationary. As a consequence of formation of solitary waves the final velocity of the last particle x_N differs from v_0. For example, $x_{20}/v_0 = 1.2338$, $x_{50}/v_0 = 1.2342$, $x_{100}/v_0 = 1.2342$. The equality of velocities $x_{50} = x_{100}$ serves as further verification of the stationary nature of a large-amplitude soliton.

Since the soliton amplitudes vary, the distance between them increases continuously. A completely similar pattern is also observed for other values of the initial velocities of the first two particles with varying time scale. It is necessary to note that for free ends of the chain ($\varphi_1 = \psi_N = 0$) there occurs a recoil of the first particles and a "destruction" of the system. For example, at the moment of time $t = 2\cdot10^{-4}$ sec, when the second soliton of lesser amplitude is located near the 27th particle, the particles from 1 to 7 have a negative velocity, and those from 1 to 8 are removed from each other by a distance larger than 2R. The velocity values of the first seven particles equal -0.11, -0.048, -0.013, -0.0068, -0.0029, and -0.0004 m/sec. The removed fractional pulse is approximately 10% of the initial value. Clearly, the "destruction" of the system at a certain moment of time will not affect the soliton shape, but the very fact of destruction renders it impossible to accurately determine the soliton amplitude from the initial conditions in any continuum description.

It follows from Eq. (3.1) and the fact of existence of stationary solitary waves that the temporal half-width of a soliton λ and its phase velocity V must depend on the particle velocity at the maximum of the solitary wave v_m as follows:

$$\lambda \sim v_m^{-1/5},\quad V \sim v_m^{1/5}.$$

The obvious difference between solitons in the given system and soliton solutions of the KdV equation is the nonlinear dependence of the propagation velocity and of the square of the reciprocal half-width λ^{-1} on the velocity amplitude v_m. It is also interesting that the spatial soliton size is in the given case independent of the velocity amplitude v_m, and equals five particle diameters. We recall that solutions of the continuum equation (2.4) in the form of solitary waves exist only for nonvanishing initial deformations ξ_0. Its final value guarantees the required asymptotic behavior of the solution for $\xi \to \xi_0$, leading to soliton formation. In a numerical calculation solitary waves also exist for $\xi_0 = 0$. In specific numerical calculations it was clarified that in the presence of initial deformations $\xi_0 \ll \xi_m$, guaranteeing the application of constant external forces to the ends of the chain, the pattern of perturbation decomposition into solitary waves does not change qualitatively with respect to the case $\xi_0 = 0$. It was also found that assignment of an initial deformation $\xi_0 \sim \xi_m$ changes qualitatively the nature of the solution.

It is interesting to compare the stationary solutions of the continuum equation (2.4) with those in a numerical account of solitary waves, being the stationary solutions of the system of equations (1.2). As already noted, the solutions of Eq. (2.4) in the form of solitary waves for deformations much larger than the initial ξ_0 are very well described by the function (2.7). The time dependence of $\delta/2R$ is shown in Fig. 3 for particles with numbers

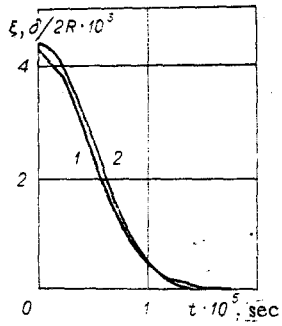

Fig. 3

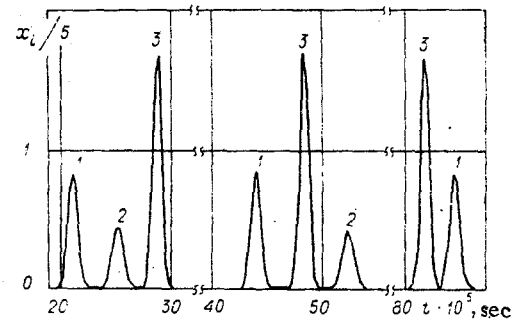

Fig. 4

60 and 61 (curve 1), obtained with a time step $0.25 \cdot 10^{-5}$ sec, as well as the function (2.7) (curve 2), in which the value of the phase velocity was taken equal to its value in the numerical account. The moment of achieving maximum deformation is reached later on. It is seen from Fig. 3 that the continuum approximation is in satisfactory agreement with the numerical calculation with $t \leqslant 10^{-5}$ sec. At the same time the difference is large for $\xi \to 0$, which is natural, since the function (2.7) does not give the correct asymptotic behavior in this region.

Also investigated was the case in which the initial velocity is communicated by the first 4 particles. In this case the perturbation was decomposed into 4 solitary waves. If the initial velocity is communicated by the single first particle, a single soliton is formed in the system.

3.2. Soliton Interaction. Two cases were investigated.

A. Collision of solitons moving toward each other. The initial velocity conditions are:

$$x_1(t=0) = x_2(t=0) = 5\,\text{m/sec}\ x_{100}(t=0) = x_{99}(t=0) = -5\,\text{m/sec}$$
$$x_i(t=0) = 0,\ i \neq 1,\ 2,\ 100,\ 99,\ N = 100.$$

The ends of the chain are assumed free. The result of the collision is shown in Fig. 2, where it is seen that initially there is a decomposition into 4 solitons, moving toward each other. Until the collision each of the pairs is displaced similarly to the case 3.1. Following the interaction, the solitons do not change their shape. Only phase changes occur. The difference in the arrival time of the first velocity maximum at the 75th particle between case A and the corresponding case 3.1 is around 10 μsec (see Fig. 2). A similar soliton interaction without a change in their shape was observed by us during reflection from a rigid wall of a sequence of 6 solitary waves, generated by impact with a chain of particles (N = 80) by a piston with mass 5m.

B. Overtaking of a lower amplitude soliton by a larger amplitude soliton. The initial conditions for the velocity are

$$x_1(t=0) = x_2(t=0) = 10\ \text{m/sec},\ x_{18}(t=0) = x_{19}(t=0) = 5\ \text{m/sec}$$
$$x_i(t=0) = 0,\ i \neq 1,\ 2,\ 18,\ 19,\ N = 150.$$

The ends of the chain are free: $\varphi_1 = \psi_N = 0$. In particular, the leading group of the solitary waves 1-3, shown in Fig. 4, were formed for the choice of initial conditions in the system. The time interval $2 \cdot 10^{-4} < t < 3 \cdot 10^{-4}$ sec corresponds to the velocity graph of the 50th particle, the interval $4 \cdot 10^{-4} < t < 5.5 \cdot 10^{-4}$ sec – to the velocity graph of the 85th particle, and the interval $t > 8 \cdot 10^{-4}$ sec – to the velocity of the 145th particle. In the latter case soliton 2 is not shown, since even for $t > 5 \cdot 10^{-4}$ sec it does not participate in the interaction between solitons of a given group. It is seen from Fig. 4 that soliton 3 is subsequently passed by solitons 2 and 1. The amplitude and shape of the solitary waves did not change in this case. It is interesting that for these initial conditions 6 solitary waves formed in the system, despite the fact that the initial perturbation, consisting only of 2 moving particles, decomposes into 2 solitons (Section 3.1). The fact given is a consequence of the nonlinear nature of the particle interaction.

3.3. Action of External Force of Triangular Profile. The initial conditions for the velocity are:

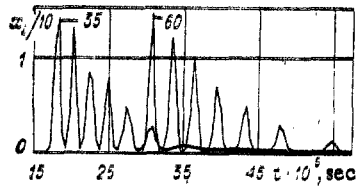

Fig. 5

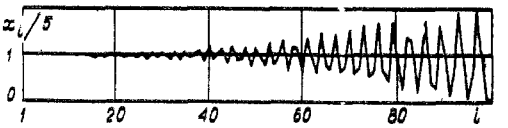

Fig. 6

$$x_i(t=0)=0,\ N\geqslant i\geqslant 1,\ N=100.$$

The force acting on the left end of the chain was given as follows:

$$\varphi_1=2\cdot 10^6(1-10^4t)\ \text{m/sec}^2,\ 0\leqslant t\leqslant 10^{-4}\text{sec};\varphi_1=0,\ t>10^{-4}\ \text{sec}.$$

The right end of the chain is assumed free ($\psi_N - 0$).

It is seen from Fig. 5, where the velocities of the 35-th and 60-th particles are shown, that the perturbation decomposed into 7 solitons. For decreasing time of force action down to 10^{-5} sec the number of solitons decreased to one. The pulse durations of 10-100 μsec are typical of blast experiments. Therefore the discrete structure of the granular medium appears to have a substantial effect on the formation of pulse compression in this case.

3.4. The Piston Problem. The initial conditions for the velocities are:

$$x_1(t=0)=5\ \text{m/sec},\ x_i(t=0)=0,\ N\geqslant i>1,\ N=200.$$

The right end of the chain is assumed free ($\psi_N = 0$), while the left end is subject to the condition $\varphi_1=\psi_2$, guaranteeing constancy of the first particle velocity.

The values of all particle velocities at moment of time $t = 5.45\cdot10^{-4}$ sec are given in Fig. 6. For convenience of perception the velocity values of neighboring particles were interpreted as a union of straight lines. The real velocity values correspond only to integers. The amplitude of the first maximum v_m approaches with time twice the value of the piston velocity v_0. This result is similar to those obtained for a Toda chain [6], for particles mutually interacting according to the Morse potential [7], and for the nonlinear KdV equation [8]. It is also seen from Fig. 6 that a soliton with a velcoity amplitude equal to $2v_0$ is formed with the flow of time at the head of the wave. The motion of the medium does not merge on the stationary regime, despite the practical constancy, starting with i = 20, the velocity of the leading front equal to the soliton velocity with an amplitude $2v_0$, and the achievement of a stationary state by particles near the piston. The nonstationarity of motion consists of a continuous increase in the number of particles participating in the oscillatory motion. It is necessary to note that the velocity of the leading front gets near the velocity of the established soliton with an accuracy of 1% already at the first ten particles. Therefore, fixing in the experiment only the velocity of the leading front, one can reach erroneous conclusions concerning process stationarity.

It is interesting to compare the velocity of the leading front of a nonstationary wave V with the velocity D_1 of a stationary impact wave, propagating in the given case in the presence of dissipation. Starting from the equations of state of the medium and the mass and momentum conservation equations, we find that

$$D_1=\left(\frac{2E}{(1-\nu^2)\pi\rho_0}\right)^{2/5}v_0^{1/5}.$$

Using the numerical results, we obtain that the soliton phase velocity V with maximum velocity v_m equals

$$V\approx 0.915\left(\frac{2E}{(1-\nu^2)\pi\rho_0}\right)^{2/5}v_m^{1/5}.$$

For $v_m = 2v_0$ we have a ratio $V/D_1 \simeq 1.05$.

Thus the difference between the established velocity of the leading front of a nonstationary wave and a stationary wave is ∿5%. The given difference renders the possibility of

estimating an experiment only from the leading front velocity unreal unless we are in the stationary regime.

If there are dissipative losses in the medium, then if they are small it is natural to expect (by analogy with the KdV equation) that the shape of the leading front of the wave is near a soliton shape. Its amplitude v_{m1} must guarantee the front velocity, equal to D_1. Using the expression for the soliton velocity, we find from this requirement

$$v_{m1} \simeq 1.56\, v_0.$$

Thus, for small dissipation the mass velocity at the stationary front can exceed the piston velocity by 1.56 times. It is interesting that the ratio found v_{m1}/v_0 coincides with the values of ξ_m/ξ_c, obtained from the continuum treatment (sec. 2). It was found in [6, 7] that for a sufficiently large index of nonlinearity the particles near the piston carry out undamped oscillations. Unlike these two cases, it was found in our numerical experiment that the velocity profiles in the coordinates $w_i - i$ are identical for the values $v_0/V = 0.95$ and $5\cdot10^{-3}$ at the corresponding moments of time, which is in agreement with Eq. (3.1). It follows from the dependence of the shock wave velocity on v_0 that the impact adiabat of the granular medium is independent of the size of the powder particles, as is the front velocity for nonstationary wave motion in the absence of dissipation.

We now turn our attention to the energy distribution in the system between kinetic E_k and potential E_p energies. The ratio $E_k/E_p = 1.249$ is established by the time $t \approx 3\cdot10^{-5}$ sec, when primarily 6 particles participate in the motion. It follows that E_k/E_p is practically constant. The maximum deviation from this value does not exceed 0.8%. The given value of E_k/E_p is near the expected one by the virial theorem for particles interacting according to the Hertz law and performing finite oscillatory motion:

$$\langle E_к \rangle = -\frac{1}{2}\left\langle \sum_i \mathbf{r}_i \mathbf{F}_i \right\rangle \Rightarrow \frac{\langle E_к \rangle}{\langle E_p \rangle} = 1.25.$$

It does not follow from the virial theorem, however, that deviations from the mean value will be small, as is observed in the numerical calculation. The smallness of deviations from mean values is, obviously, explained by the large number of particles in the system. A similar energy distribution between E_k and E_p was also observed in cases 3.1 and 3.2.

We also note a feature observed in the numerical calculation. Since the velocity amplitude of the soliton peak increases, approaching $2v_0$, the value of the maximum velocity of the last particle v_N will exceed $2v_0$. The values of v_N/v_0 for N = 20, 50, 100, and 200 equal, respectively, 2.708, 2.836, 2.876, and 2.895. As already noted, the ratio v_N/v_0 is independent of v_0.

The results of the calculation show that in the problem under consideration the pressure in the maximum of the first oscillator p_m substantially exceeds the pressure established near the piston p_c. For example, for a piston velocity $v_0 = 5$ m/sec at the moment of time the wave front is found at the 50th particle, $p_m/p_c = 2.24$. We recall that on the basis of the continuum approximation for the stationary shock wave the pressure ratio may reach the value $p_m/p_c = 1.95$. Thus, the pressure in the shock wave at the nonstationary portion can exceed the pressure at the front of the stationary wave.

3.5. Perturbation Propagation in a Chain of Varying Radius Granules. The particle radii R_i were assigned by us by using a sequence of random numbers in the interval (0, 1), found by means of the standard program RAND:

$$R_i = \{R_0 + \mathrm{RAND}(1,0)\}10^{-3}\ \mathrm{m}.$$

A. The Piston Problem. The initial and boundary conditions are similar to the case 3.4. The velocity profile for $R_0 = 0.5$ (at the moment of time $t = 3.8\cdot10^{-4}$ sec), corresponding to the piston velocity $v_0 = 5$ m/sec, is given in Fig. 7a. Figure 7b shows the velocity of the 25th particle as a function of time for $R_0 = 0.5$ and for the same piston velocity. The radius of this particle is $7.82465\cdot10^{-4}$ m. The values of the constants equal $E = 2\cdot10^{11}\ \mathrm{N/m^2}$ $\rho_0 = 7.8\times10^3\ \mathrm{kg/m^3} \nu = 0.29$. The most important differences between the system with different particle sizes and the case when their sizes are identical (see Fig. 6) are the following.

1. In a system with chaotic particle sizes (Fig. 7a) no uniform state in velocities is reached even near the piston, unlike the case of identical sizes (see Fig. 6) for the number

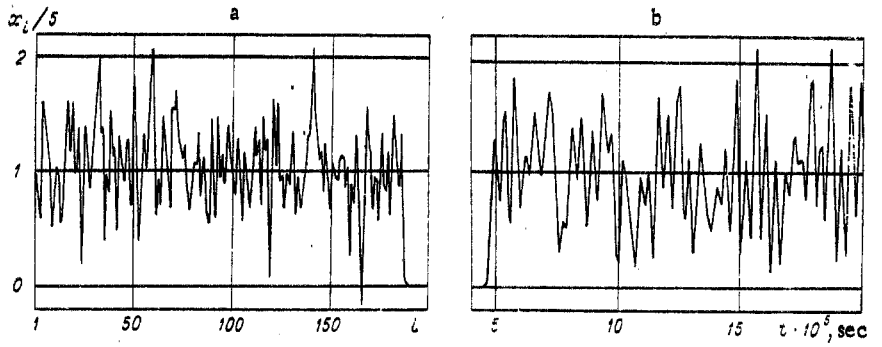

Fig. 7

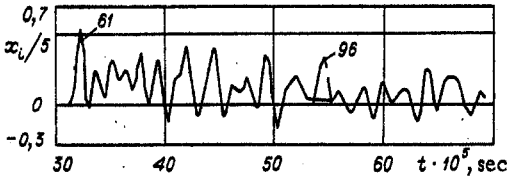

Fig. 8

of particles investigated by us N = 200. The given feature is also characteristic of the cases $R_0 = 2$ and 3 at the same piston velocity of 5 m/sec.

2. The velocity amplitude at the front can be lower than its value behind the front (Fig. 7a, b), and does not tend monotonically to the value of half the piston velocity. The value of the particle velocity in the first leading oscillation varies with the propagation into the material in a nonmonotonic way, and can be both smaller than v_0 and substantially exceed this value. In this case the smallest particle mass does not necessarily correspond to a high velocity in the first maximum, and conversely. Behind the wave front different particles can reach velocity values larger than $2v_0$ (see Fig. 7a, b). Particle velocities larger than $2v_0$ were determined in all three investigated cases with $R_0 = 0.5$, 2, 3 for a piston velocity $v_0 = 5$ m/sec. The excess of individual particle velocities over $2v_0$ increased with decreasing R_0, i.e., with the increase in spread in values of particle sizes and masses. The maximum velocity value behind the front 11.76 m/sec was fixed at the 25th particle with $R_0 = 0.5$, $v_0 = 5$ m/sec. The wave front is at this moment at the 170th particle. A feature of the problem with chaotic particle sizes is also the appearance of negative velocities. For example, in the problem with $R_0 = 0.5$, $v_0 = 5$ m/sec the same 25th particle had a velocity of -2.142 m/sec. The wave front was at this time at the 148th particle.

When the perturbation emerges from the free ends of the chain, the final velocity for the last particle is for $R_0 = 2$ less than in the case of identical particles. For example, $v_{100}/v_0 = 2.366$, distinctly from the value 2.876 for the case of identical particles. At the same time, for $R_0 = 0.5$ $v_{100}/v_0 = 2.969$, which is larger than the similar velocity ratio in the case of identical particles.

Thus, although the chaotically varying particle size causes disordered oscillations of their velocities behind the front, the nonlinearity of the interaction can also lead in this case to substantial excess of the velocity amplitude at the front and behind it in comparison with the piston velocity.

3. The ratio of kinetic to potential energies in a system with varying particle size also contains oscillations near the mean value, as is the case for a system with identical particle sizes. The differences between these two cases are that the maximum deviations from the mean value are substantially larger in the first case, and the mean values of E_k/E_p differ by more from the value 1.25, following from the virial theorem. For example, the values of E_k/E_p, averaged over the time interval during which the leading front of the wave traverses the distance from the 70th to the 90th particle for the cases $R_0 = 0.5$, 2, and 3, equal, respectively, 1.178, 1.236, and 1.232. In this case the maximum relative deviations from these mean values equal, respectively, 9, 7, and 6%.

B. Decomposition of an Initial Perturbation in a Chain of Granules with Free Ends. The initial conditions are similar to the case 3.1.

The time dependences of the velocities for the 61st and first oscillations of velocity for the 96th particle are given in Fig. 8 ($R_0 = 2$). Compared with the case of identical particles, the perturbation does not decompose now into 2 solitons, but has a significant amount of random character. At the same time it is characteristic that the leading perturbation can be near in shape to a soliton, and decay in amplitude even in the absence of dissipative losses. It is seen from Fig. 8 that this damping is related to scattering of energy by a large number of particles. The velocity amplitude damping is conveniently traced by the maximum velocity v_N of the last particle. Thus, for $R_0 = 0.5$ $v_{100}/v_0 = 0.692$, for $R_0 = 2$ $v_{100}/v_0 = 0.507$, and for $R_0 = 3$ $v_{50}/v_0 = 1.003$. It is seen that these values are substantially smaller than 1.2342, characteristic of a system of identical particles (see Sec. 3.1). It is interesting that here, as in the piston problem considered in the preceding section, a significant increase in the amount of particle chaotization in size does not lead in the transition from $R_0 = 2$ to $R_0 = 0.5$ to an enhanced damping of the velocity amplitude. On the contrary, damping is smaller in the case with $R_0 = 0.5$. In conclusion we enumerate the basic results:

1. The existence of solitary waves of new type was observed by numerical methods for properly packed spherical granules.

2. The reaction of the given system to various perturbations was investigated. The interaction of solitons and their basic properties and features were studied.

3. It was found that the continuum equation of a nonlinear chain of oscillators, being a long-wave approximation, has stationary solutions in satisfactory agreement with numerical calculations.

4. The basic features of perturbation propagation in systems with chaotically varying granule sizes were investigated.

The author is grateful to L. V. Ovsyannikov, A. A. Deribas, and R. M. Garipov for discussing the results, and to V. V. Deineko, L. N. Shcheglov, and N. G. Annikov for assistance in performing the numerical calculations.

LITERATURE CITED

1. G. Deresevich, "Mechanics of a granular medium," in: Problems in Mechanics [Russian translation], IL, Moscow (1961).
2. G. I. Chernyi, "Propagation of planar compression waves in a granular elastoplastic medium," in: Blasts in Porous and Dispersive Media [in Russian], Naukova Dumka, Kiev (1969).
3. L. D. Landau and E. M. Lifshitz, Theory of Elasticity, Pergamon Press.
4. E. Fermi, J. R. Pasta, and S. M. Ulam, Collected Works of Enrico Fermi, Vol. 2, Chicago (1965).
5. D. H. Tsai and C. W. Beckett, "Shock wave propagation in cubic lattices," J. Geophys. Res., 71, No. 10 (1966).
6. T. G. Hill and L. Knopoff, "Propagation of shock waves in one-dimensional crystal lattices," J. Geophys. Res., 85, No. B12 (1980).
7. D. F. Strenzwik, "Shock profiles caused by different end conditions in one-dimensional quiescent lattices," J. Appl. Phys., 50, No. 11 (1979).
8. I. A. Kunin, Theory of Elastic Media with a Microstructure [in Russian], Nauka, Moscow (1975).